RNA (1998), *4*:1203–1215. Cambridge University Press. Printed in the USA.

Structure and stability of variants of the sarcin-ricin loop of 28S rRNA: NMR studies of the prokaryotic SRL and a functional mutant

KATHY SEGGERSON[1] and PETER B. MOORE[1,2]

[1]Department of Molecular Biophysics and Biochemistry, Yale University, New Haven, Connecticut 06520-8107, USA
[2]Department of Chemistry, Yale University, New Haven, Connecticut 06520-8107, USA

ABSTRACT

NMR has been used to examine the conformational properties of two variants of the sarcin-ricin loop (SRL) from eukaryotic 28S rRNA, which is essential for elongation factor interactions with the ribosome: (1) its bacterial homologue, which lacks two of the bases that flank the conserved 12-nt sequence in the middle of the SRL, but which is functionally equivalent, and (2) a functionally active variant of the eukaryotic SRL in which the bulged G within the conserved sequence is replaced by an A. The data indicate that, although the bacterial SRL is less stable than the eukaryotic SRL, its conformation is closely similar. Furthermore, even though replacement of the bulged G in the SRL with an A seriously destabilizes the center of the loop, its effect on the overall conformation of the SRL appears to be modest. In the course of this work, it was serendipitously discovered that at neutral pH, the C8 proton of the bulged G, in both PRO-SRL and E73, exchanges about 10 times faster than it does in GMP.

Keywords: alpha-sarcin; bulged G; ricin; 23S rRNA; structure

INTRODUCTION

The sarcin-ricin loop (SRL) of large subunit ribosomal RNA is an essential part of the ribosome. It consists of nt 2653–2667 in *Escherichia coli* 23S rRNA and nt 4316–4332 in rat 28S rRNA, and it includes a 12-nt sequence, AGUACGAGAGGA, that is conserved in all ribosomal RNAs. The loop is named for α-sarcin and ricin, two protein toxins that kill eukaryotic cells by catalyzing the cleavage of bonds within this sequence. This is lethal because neither elongation factor 1α nor elongation factor 2 interact normally with a ribosome when its SRL has been modified by either toxin, and hence protein synthesis fails (Fernandez-Puentes & Vasquez, 1977).

The solution structure of E73, a 29-nt RNA containing the rat 28S rRNA SRL sequence, was determined five years ago by NMR (Szewczak et al., 1993; Szewczak & Moore, 1995), and its crystal structure was solved last year (C.C. Correll, A. Munishkin, Y.-L. Chan, Z. Ren, I.G. Wool, & T.A. Steitz, in prep.). As the schematic diagram of E73 in Figure 1 shows, its most interesting feature is a bulged nucleotide, G10 (G2655 in *E. coli* 23S rRNA, 4319 in rat 28S rRNA) that reaches across the major groove and interacts with the phosphate backbone of the opposite strand. Adjacent to G10 is a reversed Hoogsteen U-A base pair, U11–A20, followed by a side-by-side A-G base pair, which together generate a cross-strand adenine stack (Wimberley et al., 1993; Correll et al., 1997; Dallas & Moore, 1997). A GNRA tetraloop closed by a C-G base pair (C13–G18) caps the loop (Heus & Pardi, 1991). [Note that E73 numbering is adhered to throughout this study.]

In this paper, we present the results of NMR studies of two variants of E73: PRO-SRL and G10A. PRO-SRL is a 27-nt RNA containing the prokaryotic SRL sequence, which differs from the eukaryotic SRL in lacking C8 and A21, which are shaded dark gray in Figure 1. The sequence of G10A is identical to that of E73 except that an adenine replaces G10. PRO-SRL is of interest because most biochemical and genetic studies on the SRL have been done in prokaryotes, not eukaryotes, and so it is important to verify that the structure of PRO-SRL is the same as that of E73. G10A is important because, even

Reprint requests to: Peter Moore, Department of Chemistry, Yale University, P.O. Box 208107, New Haven, Connecticut 06520-8107, USA; e-mail: moore@proton.chem.yale.edu.

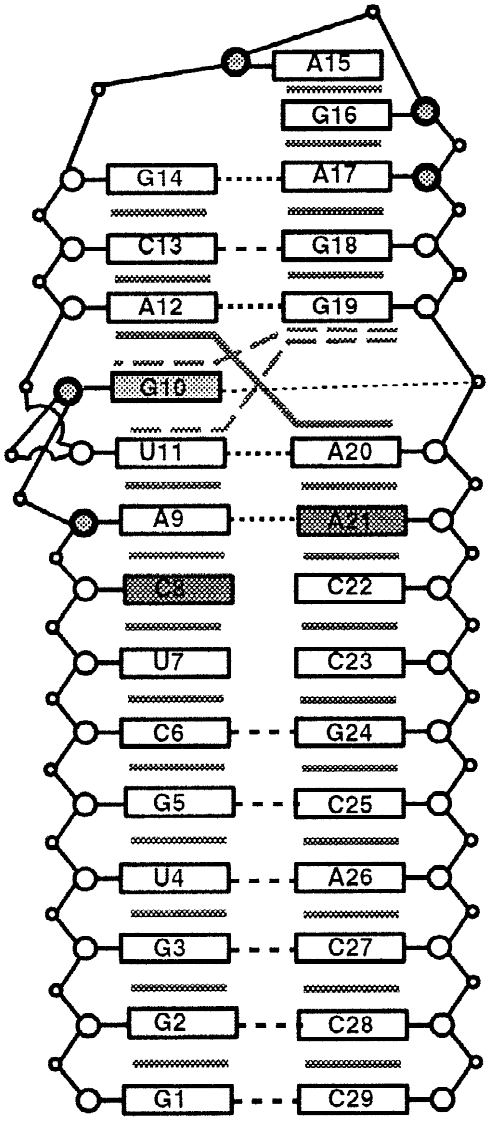

FIGURE 1. Schematic diagram of E73. Gray bars indicate stacking between bases. Extended gray bar between A12 and A20 represents the cross-strand stacking of these bases. Dotted gray bars indicate partial stacking of G19 on G10 and U11. Dotted lines between bases indicate base pairing, or in the case of G10, hydrogen bonding with the phosphate backbone. Small circles indicate phosphate groups; large circles, ribose rings, which are shaded if the sugar pucker is at least partially 2′ endo. Nucleotides that are absent from the PRO-SRL molecule (C8, A21) are shaded dark gray. Nucleotide G10, which is shaded light gray, is changed to an A in the G10A sequence. The 12-base conserved sequence corresponds to A9–A20. Alpha-sarcin cleaves the phosphodiester bond between G16 and A17. Ricin depurinates A15.

though G10 plays a vital role in the conformation of the SRL and is an identity element for its interaction with EF-G (Munishkin & Wool, 1997) and α-sarcin (Gluck & Wool, 1996), cells that contain this variant of the SRL sequence are viable. The growth rate of cells containing the G10A sequence is nearly indistinguishable from that of normal cells, but in competitive growth experiments against normal cells, G10A cells lose out (M. Macbeth & I. Wool, pers. comm.).

The data show that PRO-SRL has a conformation that is closely related to that of E73, as expected, and suggest that G10A may be similar. Surprisingly, the loop of PRO-SRL is substantially less stable than that of E73, and that of G10A so much less stable that it was difficult to characterize its conformation at all. The differences in the stability of these loops, all of which are equally competent in protein synthesis, reopens the question of whether or not the conformation of the SRL varies during protein synthesis (Nierhaus et al., 1992; Wool et al., 1992). In the course of this work, it was found that the unusual conformation of G10 causes its H8 proton to exchange with solvent more rapidly than the H8 proton in GMP, an observation that has no precedent we could identify.

RESULTS

Thermal properties of E73, PRO-SRL, and G10A

Figure 2 compares the responses of the imino proton spectra of E73, PRO-SRL, and G10A to changes in temperature. At 5 °C, the three are similar. Each contains a cluster of reasonably narrow resonances between 14 and 12.5 ppm, and a handful of broader resonances between 12.0 and 10 ppm. As the temperature increases, the upfield resonances disappear and most of the downfield resonances persist. Because the spectrum of E73 was assigned previously (Szewczak et al., 1993), and we have assigned the downfield spectra of both PRO-SRL and G10A (see below), these observations are easily interpreted. The upfield resonances in the imino proton spectra of the three molecules are loop resonances, as are the downfield resonances that are thermolabile. The thermally stable downfield imino proton resonances originate in their base paired stems. Clearly, the loops of all three molecules melt at significantly lower temperatures than their stems, and the loop of E73 is more stable than that of PRO-SRL, which in turn is more stable than that of G10A.

The optical melting profiles of these molecules are consistent with their imino spectra. Figure 3a, b, and c shows the first derivative melting curves for E73, PRO-SRL, and G10A, respectively. All three molecules display a weak, low-temperature transition around 30 °C that could be due to intermolecular associations, but they may represent inaccuracies in determining the low-temperature baseline. The larger transition at 54 °C in PRO-SRL and the corresponding 37 °C transition in G10A probably represent the melting of the loop regions of the two molecules. The 70 °C transition seen in both molecules must come from the melting of their Watson–Crick stems. As Figure 3a shows, the first-derivative curve for E73 can also be decomposed into

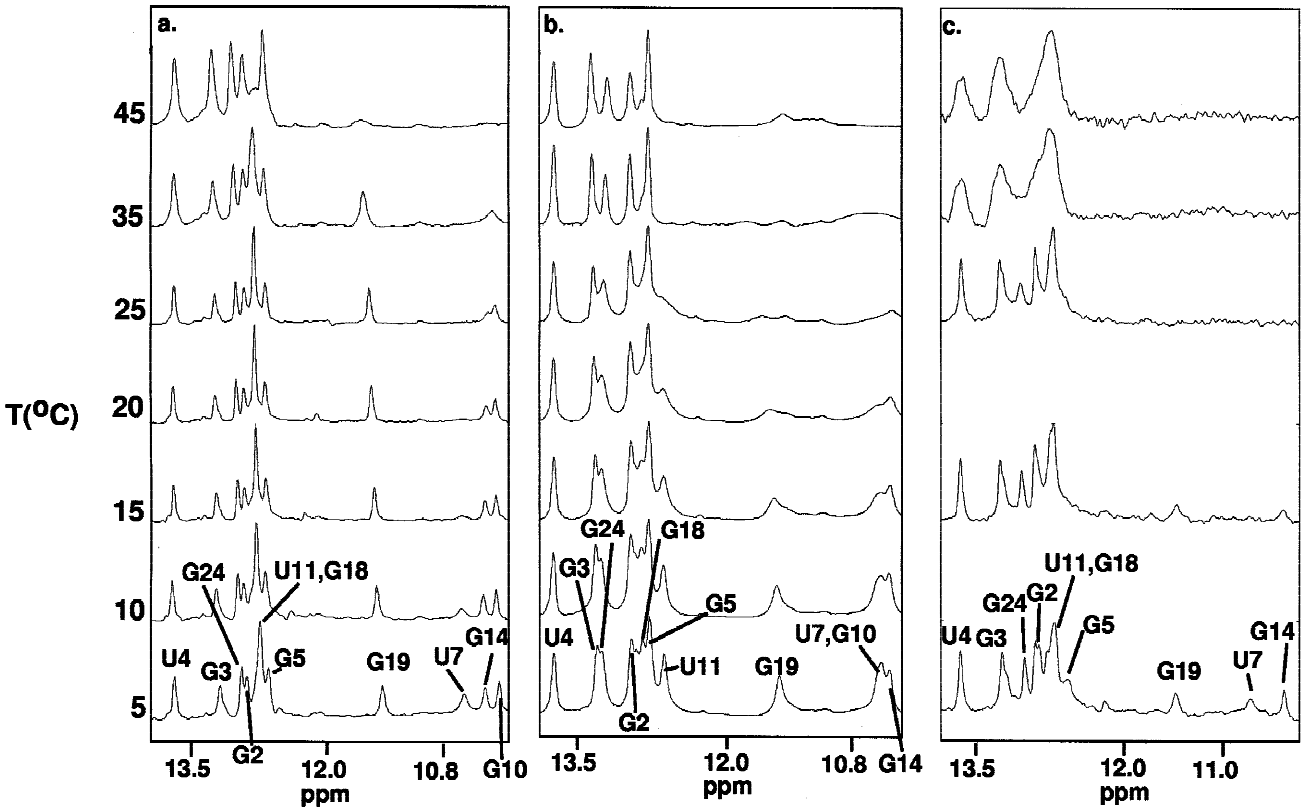

FIGURE 2. Imino temperature series of E73, PRO-SRL, and G10A are shown in **a**, **b**, and **c**, respectively. E73 and G10A spectra were taken using jump-return spin-echo water suppression sequence. PRO-SRL spectra were taken using twin-pulse water suppression.

two transitions. The transition at 70 °C probably represents the melting of E73's stem, and the transition at 58 °C, the melting of its loop. Melting profiles of all three molecules were independent of concentration, indicating that they are monomeric stem-loops under the ionic conditions chosen.

Assignment of the spectrum of PRO-SRL

Figure 4a and b shows portions of two constant-time HSQC spectra taken using ^{13}C-^{15}N labeled PRO-SRL, one of them (Fig. 4a) collected to emphasize ribose ^{1}H-^{13}C correlations and the other (Fig. 4b) collected to emphasize aromatic ^{1}H-^{13}C correlations. The information about the chemical identities of the protons responsible for resonances provided by these spectra made it possible for us to work out the anomeric–aromatic walk in the NOESY spectrum of PRO-SRL (Fig. 5), which enabled us to assign the molecule's aromatic and anomeric resonances. Once these assignments were in hand, the imino proton resonances of PRO-SRL could be assigned on the basis of NOEs between imino protons and nonexchangeable protons, and from information extracted from an ^{15}N-HMQC spectrum, which enabled us to distinguish UN3 from GN1 resonances (data not shown). A set of assignments resulted that included all of the imino, aromatic, anomeric, and H2′ resonances of the molecule, and about 80% of its H3′ resonances.

On the chemical shift of G10 C1′

G10 is the most puzzling residue, spectroscopically, in the SRL. For example, the proton responsible for the $^{1}H/^{13}C$ correlation seen at (6.00 ppm, 81.3 ppm) in Figure 4a, which the anomeric–aromatic walk indicates must belong to G10, could either be an H4′ proton with an unusually far downfield proton chemical shift, or a normal H1′ proton bonded to a C1′ carbon with an unusually far upfield chemical shift. This same correlation is seen in E73, and it was assigned to G10H1′/C1′ (Szewczak et al., 1993; Szewczak & Moore, 1995). That this assignment is correct is proven here. In a constant-time HSQC experiment taken of a fully ^{13}C-labeled RNA, the sign of a ^{1}H-^{13}C crosspeak depends on the number of carbons bonded to the carbon responsible for it. In this case, the experiment was set up so that carbons bonded to a single carbon atom (C1′ and C5′) would give negative peaks, whereas peaks due to carbons bonded to two carbons (C2′, C3′, and C4′) would be positive. Because the peak in question is negative, it must represent a 1′ carbon–proton pair.

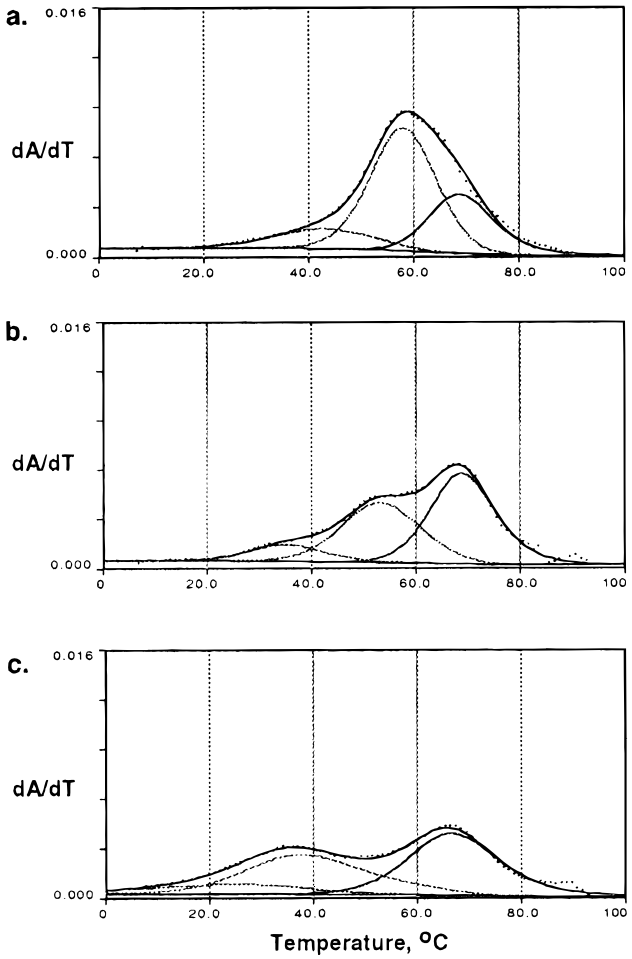

FIGURE 3. First-derivative melting curves of E73, PRO-SRL, and G10A. These curves show the first derivative of the UV absorbance melting profile of each molecule as the sum of individual two-state transitions. Dotted line in each curve represents the actual first-derivative data; solid line is the sum of the individual single transition curves. For E73, the melting temperatures for the three transitions were 43, 58, and 69 °C, and their enthalpies were 32, 48, and 55 kcal/mol, respectively. For PRO-SRL, the melting temperatures for the three transitions were 35, 53, and 69 °C, and their enthalpies were 41, 42, and 56 kcal/mol, respectively. For G10A, the melting temperatures for the three transitions were 25, 37, and 67 °C, and their enthalpies were 14, 21, and 40 kcal/mol, respectively. These plots were produced using MeltFit (Draper & Gluick, 1995).

G10 H8 proton exchange

Another puzzling property of G10 was the absence of a resonance that might correspond to G10 H8 in the spectra of E73 (Szewczak & Moore, 1995). In the aromatic constant-time HSQC spectra of PRO-SRL (Fig. 4b), we noticed an H8 resonance at 8.15 ppm in the proton dimension, which was present in the first few spectra obtained, but which was absent from spectra taken a few weeks later using the same sample. No such resonance was reported earlier for E73 (Szewczak & Moore, 1995). Because the proton resonance in question is also associated with a weak aromatic–anomeric NOE crosspeak involving G10 H1′ (6.00 ppm), we assigned the HSQC peak at 8.15 ppm to G10 H8. Because the HSQC and NOESY spectra in question were taken using samples dissolved in D_2O, we surmised that the tendency of G10 H8 resonances to disappear from spectra might be due to proton exchange with solvent.

In order to test this hypothesis, a sample of E73 that had been incubated for a prolonged period in H_2O was transferred into D_2O, and three NOESY spectra were taken of it over the course of six weeks (see Materials and Methods). The initial NOESY spectrum of E73 included a crosspeak at 5.99 ppm/8.13 ppm, corresponding to the peak in the NOESY spectrum of PRO-SRL (Fig. 6a) and, by the time the third spectrum was taken, after incubating at 30 °C for 48 h, it had all but disappeared. Based on these data, the rate constant for exchange of G10 H8 in E73 was estimated to be 0.017 h^{-1} at 30 °C. A series of HMQC experiments done with PRO-SRL yielded a similar rate constant: 0.016 ± 0.003 h^{-1} (Fig. 6b).

The rate of exchange of the H8 in GMP was also determined at several temperatures, in the same buffer used here for NMR experiments. The logarithm of the rate constant for GMP exchange was found to be linear with the reciprocal temperature, and expressing that rate as $k = A\exp(-E_a/RT)$, A was determined to be $2.62 \times 10^{14} \pm 1.8 \times 10^{14}$ h^{-1}, and E_a to be 23.8 ± 0.5 kcal/mol. Using this information, the rate constant for GMP H8 exchange in NMR buffer at 30 °C, which is too slow to be conveniently measured directly, was estimated to be 0.0018 h^{-1}, consistent with the GMP exchange measurements made previously by Lane and Thomas (1979) using laser-Raman spectroscopy under similar conditions. Thus, the rate of exchange of G10 H8 in both E73 and PRO-SRL is about 10 times faster than the rate of H8 exchange of free GMP.

Comparison of the spectroscopic properties of E73 and PRO-SRL

When the published assignments for E73 were compared with those obtained for PRO-SRL, it immediately became apparent that the two RNAs must have similar conformations. Figure 7 compares the H6/H8, H1′, and C1′ chemical shifts of the two RNAs, and it is evident that the chemical shifts of corresponding atoms in the two molecules are remarkably similar. Significant chemical shift differences are concentrated in the residues most affected by the sequence difference between the two molecules: U7, A9, C22, and A20. Because chemical shifts are highly sensitive to structure, these correlations suggest similarity of conformation.

E73 and PRO-SRL share many other spectroscopic similarities. The lack of any extremely strong H1′ to aromatic crosspeaks in the NOESY spectra of both E73 and PRO-SRL indicates that the chi angles in both

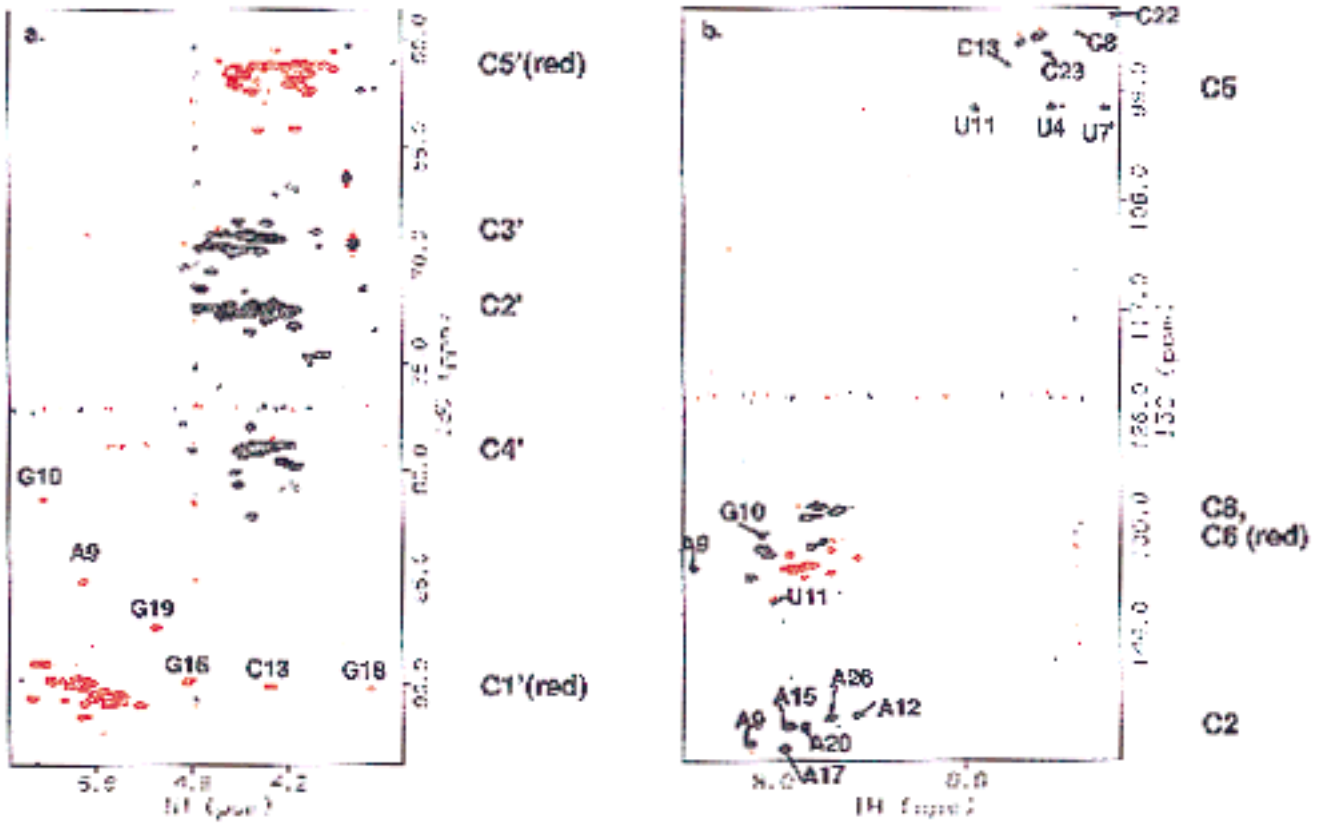

FIGURE 4. Constant time HSQC spectra of $^{15}N/^{13}C$-labeled PRO-SRL at 15 °C, taken on the Varian 600MHz spectrometer. **a:** This spectrum was collected to emphasize the anomeric region. Resonances coming from H5′-C5′ and H1′-C1′ correlations are negative and colored red. Resonances coming from H2′-C2′, H3′-C3′, and H4′-C4′ correlations are positive and colored black. Some of the one-bond correlations between H1′-C1′ nuclei are identified, including resonances unusually upfield shifted in the carbon dimension, G10 and A9, and resonances unusually upfield shifted in the proton dimension, C13 and G18. **b:** This spectrum emphasizes the aromatic region. Resonances coming from the H5–C5, H8–C8, and H2–C2 correlations are positive and colored black, and the H6–C6 are negative and colored red. For clarity, only a few of the resonance assignments are labeled.

are all *anti*. In both molecules, the strongest 1′-2′ crosspeaks observed in DQF-COSY spectra correspond to G10 and A9. The weak 1′-2′ peaks seen in the E73 DQF-COSY for G1, A15, G16, A17, and C29 were not observed in PRO-SRL, but their absence may not be significant. Resonances in the spectra of PRO-SRL are generally broader than E73 resonances, probably because of conformational exchange related to its reduced stability. This may also explain why not all of the NOEs observed in E73 were seen in PRO-SRL. In PRO-SRL water NOESY spectra, we observed a subset of the NOEs of E73, and in D_2O NOESY spectra, many crosspeaks are weaker in PRO-SRL than they were in E73.

Included among the NOEs observed in PRO-SRL spectra, however, are most of those that were important for establishing the structure of E73. For example, the imino proton NOESY spectra of PRO-SRL include an NOE between U11 H3 and A20 H8, which indicates reverse-Hoogsteen pairing between these two bases, as seen in E73. NOEs were also observed between the GH1 and AH8 resonances for two base pairs in the loop, A12–G19 and A17–G14, confirming that they are type II G-A pairs, as they are in E73. Finally, NOEs observed between the imino proton of G10 and the H2′ and H3′ of G19, which are also seen in E73, prove that G10 must reach across the major groove in PRO-SRL the way it does in E73.

As Figure 5 illustrates, the nonexchangeable NOESY spectrum of PRO-SRL is also full of correlations diagnostic of E73's conformation. For example, an NOE between A9 H1′ and U11 H6 indicates that G10 does not stack on A9, consistent with the structure of E73. There is also a strong "backward" NOE between A9 H8 and U11 H1′, indicating that the residue between them, G10, is positioned in a way that allows A9 to stack on U11, as it does in E73. In fact, the difference between the chemical shifts of A9 H1′ and U11 H1′ is greater in PRO-SRL than it is in E73, making it easier to distinguish the backward A9–U11 NOE from the normal A9 self NOE than it is in E73. Furthermore, there is a strong A12 H2–A20 H2 NOE, indicative of the pres-

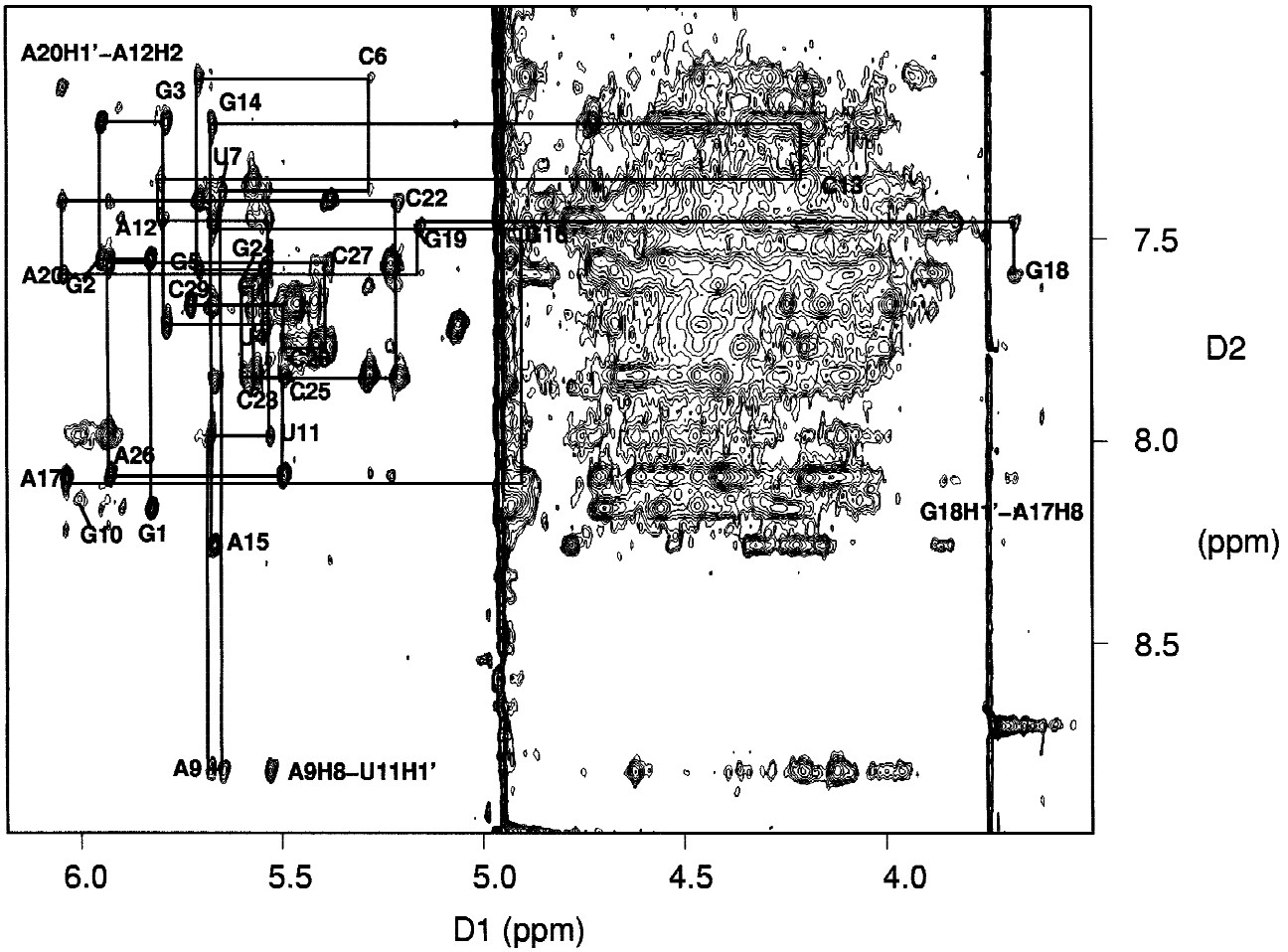

FIGURE 5. Nonexchangeable aromatic and anomeric resonances of PRO-SRL. A NOESY spectrum is shown, taken in D_2O at 5 °C with a 300-ms mixing time. The aromatic–anomeric walk from G1 to C29 is shown. At A9, the sequential walk jumps to U11. The following NOEs are also annotated: U11 H1′-A9 H8 "backward" NOE, G10 H1′-H8 self NOE, A20 H1′-A12 H2 NOE, G18 H1′-A17 H8 "backward" NOE.

ence of a cross-strand A stack in this part of PRO-SRL, as expected.

The NOEs observed involving residues in the GAGA sequence of PRO-SRL suggest that this region is a GNRA tetraloop, as expected. The extreme upfield shift of G18 H1′ at 3.68 ppm (Fig. 4a) reflects its position beneath the aromatic ring of A17, and is typical for the H1′ that belongs to the nucleotide that is 3′ of the last A in a GNRA tetraloop. An upfield shift is also observed for C13 H1′ (at 4.20 ppm) that, like G18, is 3′ of the adenine in a GA pair (A12). In both respects, PRO-SRL is E73-like.

Structural calculations on PRO-SRL

Torsion angle molecular dynamics (TAMD) calculations (Stein et al., 1997) were done using data extracted from the spectra of PRO-SRL and, as Figure 8 shows, the model that resulted for PRO-SRL closely resembles the solution structure published for E73 (RMSD 1.7 Å for residues A9–A20) (Szewczak & Moore, 1995). Only in the regions where the sequences of the two molecules differ do their structures diverge significantly.

PRO-SRL differs from E73 in the region that links the noncanonical motifs in the loop with the A-form, Watson–Crick base paired stem. In the E73 structure, there is a series of three base juxtapositions: A9–A21, C8–C22, U7–C23. In PRO-SRL, there are only two: A9–C22 and U7–C23. There is scant evidence in PRO-SRL spectra constraining the way U7–C23 and A9–C22 interact. The U imino proton is protected from exchange, which it is not in E73, and the amino group of A9 is protected from exchange in both PRO-SRL and E73, but no NOEs were observed that give further information about the pairing of these residues. However, because the residues in question, U7, A9, C22 and C23, are part of the sequential walk in PRO-SRL NOESY spectra, there must be continuous A-form-like stacking through this part of the molecule, which suggests that the U7–C23 and A9–C22 residues are juxtaposed in an ordered

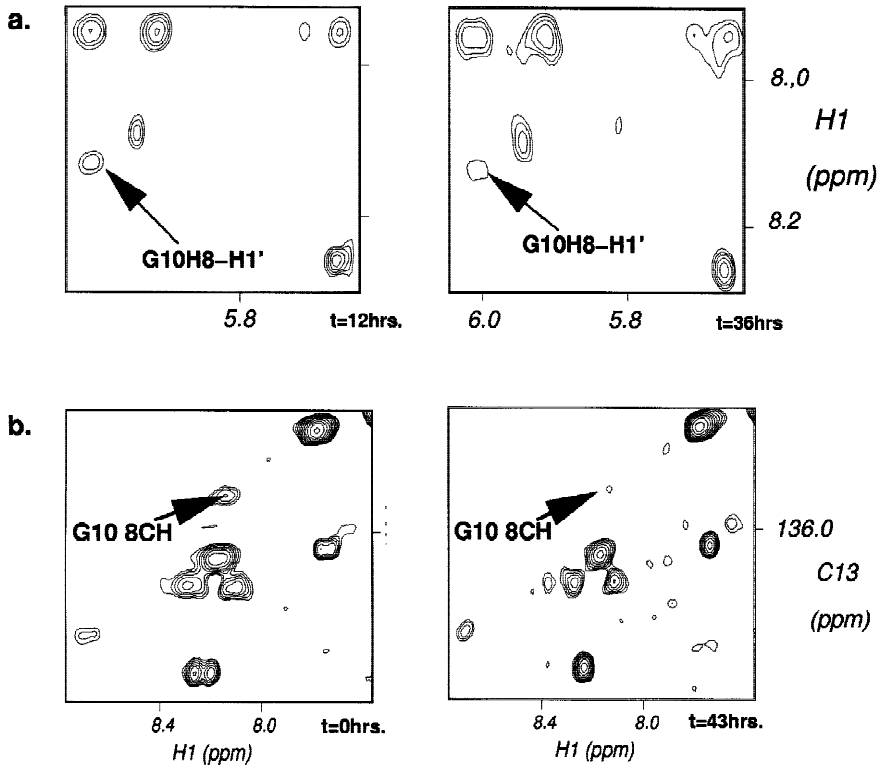

FIGURE 6. G10 H8 observed in spectra of PRO-SRL and E73. **a:** Portion of the nonexchangeable NOESY of E73 is shown with the peak due to the G10 H8–H1′ self NOE labeled. In the second spectra, which was taken after the sample had been incubating at 30 °C for 24 h, the peak intensity has diminished. **b:** Portion of the aromatic region of the constant time HMQC of $^{15}N/^{13}C$-labeled PRO-SRL is shown, with the resonance due to G10's H8–C8 correlation labeled. In the second spectrum, which was recorded 43 h later, the resonance due to G10 H8–C8 is diminished in intensity.

way. In the lowest-energy structures resulting from TAMD calculations of PRO-SRL, there was no tendency of base hydrogen bond donors on C23 to approach base hydrogen bond acceptors on U7 within hydrogen bonding distance, or vice versa. The arrangement of A9 and C22 in the lowest-energy structures was similar in this regard, with stacking interactions being the dominant interaction controlling the positions of these nucleotides. In only one of the low-energy structures computed did an A9–C22 base pair form (A9 H62–C22 N3; A9 N1–C22 H42), but this pair also had less favorable stacking interactions around A9–C22 than other structures in the family.

Assignment of the G10A spectrum

The spectra of G10A were more difficult to assign than those of either E73 or PRO-SRL, presumably because of the instability of its loop. In nonexchangeable NOESY spectra taken at 5 °C, we were able to find strong NOEs that allowed us to assign resonances from residues G1 through C6 and G24 through C29 in the stem, C13 through G18 in the tetraloop, and C22 and C23 in the loop. The remaining NOE crosspeaks, which must represent loop residues C8, A9, A10, U11, A12, A20, and A21, were either broad or very weak, and in any case, poorly connected. In so far as the resonances of these loop residues were assigned at all, they were assigned on the basis of self H1′–aromatic, H1′–H2′ and H5–H6 NOEs, and by analogy to the NOEs and chemical shifts observed for corresponding residues in PRO-SRL and E73. Figure 9 shows those parts of the aromatic–anomeric walk for G10A for which the data are most persuasive: G1 through A9, C13 through G19, and G24 through C29. Because imino proton exchange is rapid in the loop of G10A, no imino–imino NOEs were observed in the loop, and imino–other NOEs had to be relied on to assign loop imino protons. Arguments based on NOEs of this kind sufficed to assign the imino proton resonances of U11, G18, G19, and G14. An assignment was proposed for U7 H3, but it depends entirely on analogy with E73 and PRO-SRL.

Another indication of conformational exchange in the loop could be seen in the DQF-COSY spectra of G10A. Its pyrimidine H5–H6 crosspeaks vary considerably in strength, which is not the case for E73, although such variation is seen to a lesser extent in the PRO-SRL DQF-COSY (data not shown). The strong cross peaks all originate in the molecule's stem, and the weak ones come from its loop. The reason these crosspeaks are weak is that many loop resonances have transverse relaxation times that are significantly shorter than resonances in the stem. That fact was also plainly evident in one-dimensional spectra of G10A taken in D_2O. For example, the most upfield aromatic resonance in the spectrum of E73 is that of A12 H2, which, like most AH2 resonances, is exceptionally narrow, about 14 Hz, full width at half height. There is a resonance at about the same chemical shift in the spectrum of G10A, but, instead of being one of the narrowest, it is one of the

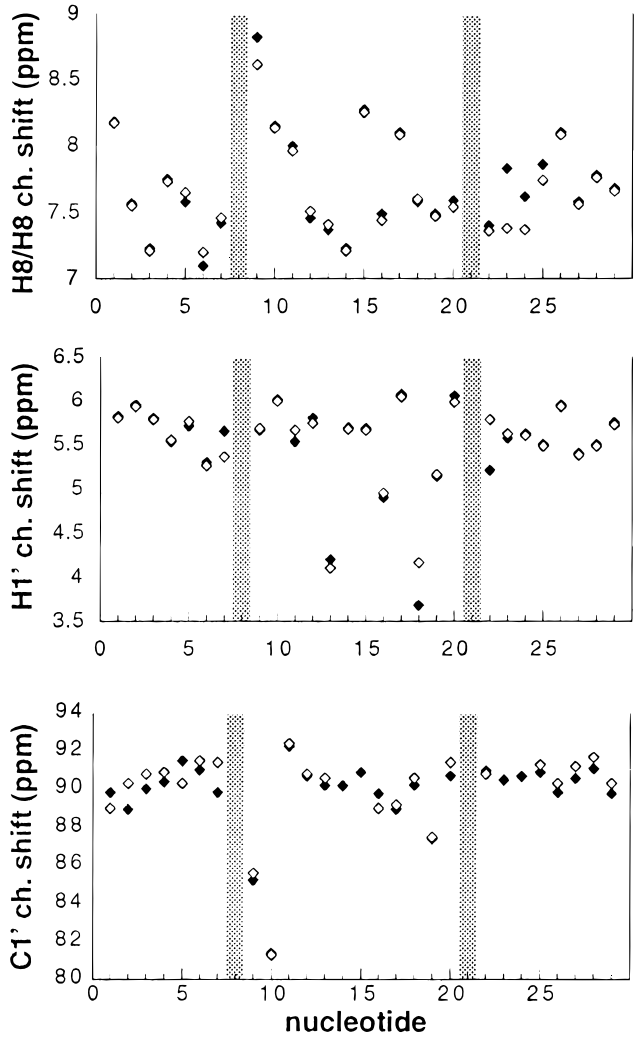

FIGURE 7. Comparison of chemical shift assignments for PRO-SRL and E73. Top graph shows the chemical shift values for resonances due to H8 and H6 protons of PRO-SRL and E73. Solid diamonds indicate PRO-SRL resonances; open diamonds indicate E73 resonances. Middle graph shows the chemical shift values for H1′ resonances. Bottom graph shows the chemical shift values for C1′ resonances. Chemical shifts of C1′ resonances from G14 and A15 in E73 were not assigned, so only PRO-SRL shifts are shown for these nucleotides. Gray bars indicate the point of sequence difference between E73 and PRO-SRL, where C8 and A21 are absent in PRO-SRL.

broadest, about 40 Hz (data not shown). In addition to making NOESY spectra uninformative, the short transverse relaxation times of many loop resonances made it difficult to learn much about the loop using ^{1}H-^{13}C correlation experiments.

Structural inferences about G10A

There can be no doubt that in G10A, G1 through C6 pairs with G24 through C29 to make an A-form double helix. All of the NOEs characteristic of A-form RNA are found associated with those residues. Nor can there be much doubt that residues C13 through G18 of G10A form a GNRA tetraloop that is closed by a C-G base pair. There are several imino to nonexchangeable proton NOEs supporting the C13–G18 base pair and a single, weak G14 imino-A17 H8 NOE showing that G14 and A17 form a type II GA pair.

The argument for the conformation of the rest of the loop is less direct. It depends on weak NOEs and chemical shift comparisons to E73. For example, Figure 10 compares the H1′ and H6/H8 chemical shifts of E73 and G10A. Because there is only a single base difference in sequence between the two molecules, and it occurs at position 10, which is several nucleotides away from the stem, the chemical shifts of stem nucleotides ought to be identical in the two molecules, provided their conformations are the same, of course. As Figure 10 shows, this is indeed the case. Even in the two shaded regions, where assignments are less secure, there is significant correlation between the chemical shifts of the two molecules. The resonances of C13 through G18 correlate closely with those coming from the same region of E73, supporting the conclusion that they also form a GNRA tetraloop in G10A. It is interesting that the linewidths of resonances originating in the C13 through G18 region of G10A are almost as narrow as its stem resonances (see Fig. 9), which suggests that the structure of the tetraloop must be reasonably stable.

The most difficult part of the G10A molecule spectroscopically is the region around A10. For lack of imino–other NOEs, we are unable to comment directly on the pairings of G19 and U11, which are critical for organizing the corresponding regions of E73 and PRO-SRL, even though the downfield spectrum of G10A includes imino proton resonances at the unusual chemical shifts characteristic of those two residues in E73 and PRO-SRL. The remarkably strong NOE between A12 H2 and A20 H2, which signals the presence of a cross-strand A stack in E73 and PRO-SRL, is barely detectable in G10A. The only one of the many spectroscopic features diagnostic of the architecture of the bulge region in E73 for which we can find any convincing trace is an NOE between A9 H1′ and U11 H6, which is indicative of the formation of the characteristic S-turn of the backbone in that region. Even the strong H1′-H2′ COSY cross peaks expected for the riboses of A9 and A10, which are C2′-endo in E73, are not observed. Nevertheless, chemical shift similarities suggest that, on average, the conformation of G10A is similar to that of E73 and PRO-SRL throughout.

DISCUSSION

It is not surprising that the conformation of PRO-SRL proved to be essentially the same as that of E73. The loop sequences of the two molecules perform the same functions in eubacterial and eukaryotic ribosomes, respectively, and in vitro they are cleaved in the same

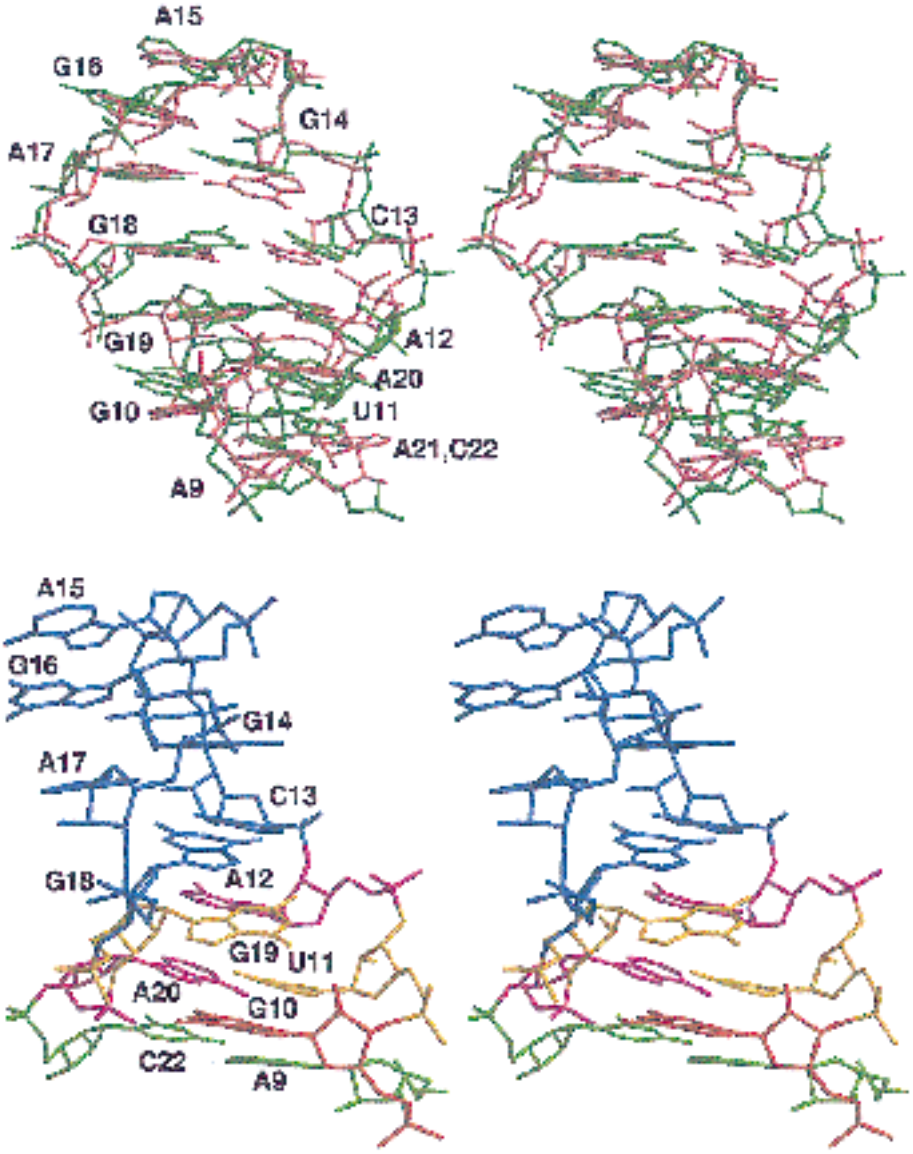

FIGURE 8. Stereo view of superposition of E73 and PRO-SRL, and TAMD PRO-SRL structural model. E73 is shown in pink and PRO-SRL is shown in green. Residues A9–A21 of E73 and A9–C22 of PRO-SRL are shown. Residues A9–A20 superimpose with an RMS difference of 1.7 Å (top). PRO-SRL model alone (bottom) is shown with its motifs color-coded. The GAGA tetraloop and its closing base pair (C13–G18) are shown in blue. Residues A12 and A20, which form a cross-strand stack, are shown in fuschia. G19 and U11, which have a partial stacking interaction, are shown in mustard. The bulged nucleotide G10 is shown in red. The base juxtaposition of A9 and C22 is shown in light green.

way by α-sarcin and depurinated similarly by ricin, both of which are sensitive to substrate conformation (Endo & Wool, 1982; Endo & Tsurugi, 1988). The principle difference between the conformation of E73 and that of PRO-SRL is that the symmetric A-A pair on the stem side of the bulged G in E73 appears to be replaced by an A-C pair that is not obviously base paired.

We note in passing that loop E of eukaryotic 5S rRNA includes a bulged G motif that is very similar to the one in the SRL (Wimberly et al., 1993). The sequences of E73, PRO-SRL, and the eukaryotic loop E are identical in that region (A9–C13, G18–A20), and the proton chemical shifts of corresponding nucleotides in the two molecules are remarkably similar.

Because organisms containing ribosomes in which the guanosine corresponding to G10 is replaced by an adenine are viable, it is plausible a priori that the loop in G10A might have a conformation similar to that of E73. The data discussed above provide significant support for the hypothesis that the distal part of the G10A loop is a GNRA tetraloop, as is the case in E73, and this inference is consistent with the observation that SRL oligonucleotides containing this substitution are substrates for ricin (Gluck & Wool, 1996), which is spe-

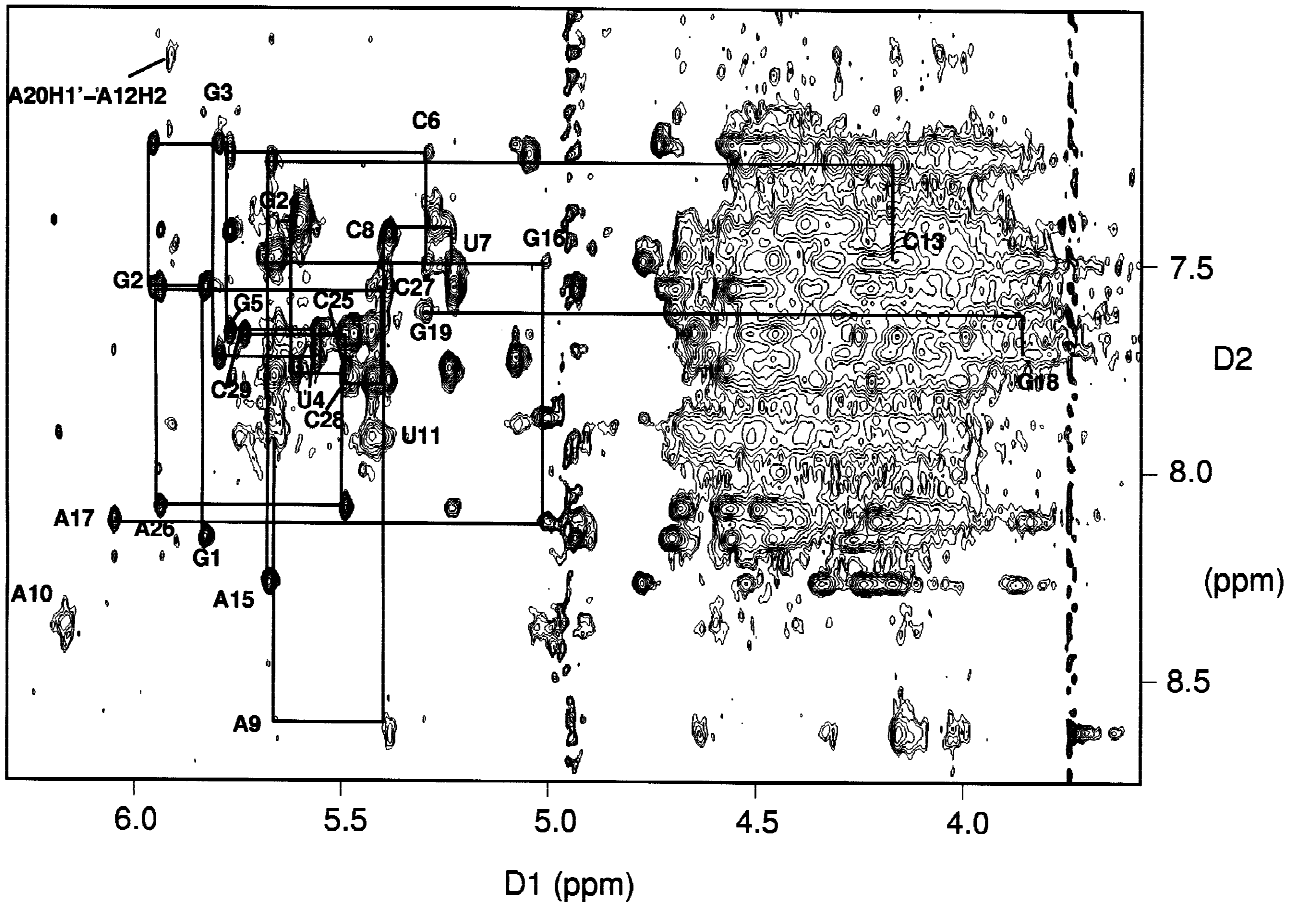

FIGURE 9. Nonexchangeable aromatic and anomeric resonances of G10A. NOESY spectrum is shown, taken in D_2O at 5 °C with a 300-ms mixing time. Aromatic–anomeric walk from G1 to A9, C13 to G19, and G24 to C29 is indicated. Also annotated are the A10 H1′-H8 self NOE and the A20 H1′-A12 H2 NOE.

cific for GNRA tetraloops having the sequence GAGA (Gluck et al., 1992). What we cannot prove is that G10A also contains the equivalent of a bulged G motif and a cross-strand A stack. The reason is that the region of the G10A loop that may contain those motifs is much less stable than the corresponding region of E73. The line-broadening seen suggests that this part of G10A is in intermediate exchange, and, because the difficulties we encountered in assigning resonances in this part of the molecule and detecting the features of its spectra that would have proven this part of G10A is the same as E73 can all be attributed to linewidth problems, the data by no means prove that the two molecules are not the same. Indeed, we believe that a conformation like that of E73 is an important component in the ensemble of conformations over which G10A averages.

Where E73, PRO-SRL, and G10A differ most obviously is in the stabilities of their loops. The destabilization that occurs in the SRL when G10 is replaced by an A is easily explained. NMR investigations demonstrated that the imino proton of G10 makes a hydrogen bond with the phosphate group that links G19 and A20, and the crystal structure of the SRL has revealed that G10 is also involved in a base triple with U11–A20, which is stabilized by a hydrogen bond between G10N3 and U11O4 (C.C. Correll, A. Munishkin, Y.-L. Chan, Z. Ren, I.G. Wool, & T.A. Steitz, pers. comm.). None of the interactions that hold G10 in position is possible for an A in the same position, and a bulged A that is unconstrained by these interactions may engage in others that are incompatible with the normal conformation of that part of the SRL. Although noticeable spectroscopically, the difference in loop stability between PRO-SRL and E73 is much smaller than that between G10A and E73, and it is correspondingly harder to be sure why it exists. It is possible that the A9–A21 pair in E73 is stronger than the A9–C22 pair that replaces it in PRO-SRL. It is also possible that the stacking interactions in E73 involving A21 are more stabilizing than those that are possible in PRO-SRL.

As pointed out earlier, the sequence of the central 12 bases of the SRL is identical in all ribosomes, and most molecular biologists would take this to imply either that its conformation is critical for protein synthesis, and/or that its sequence is read somehow during protein synthesis. In either theory, sequence changes in the SRL

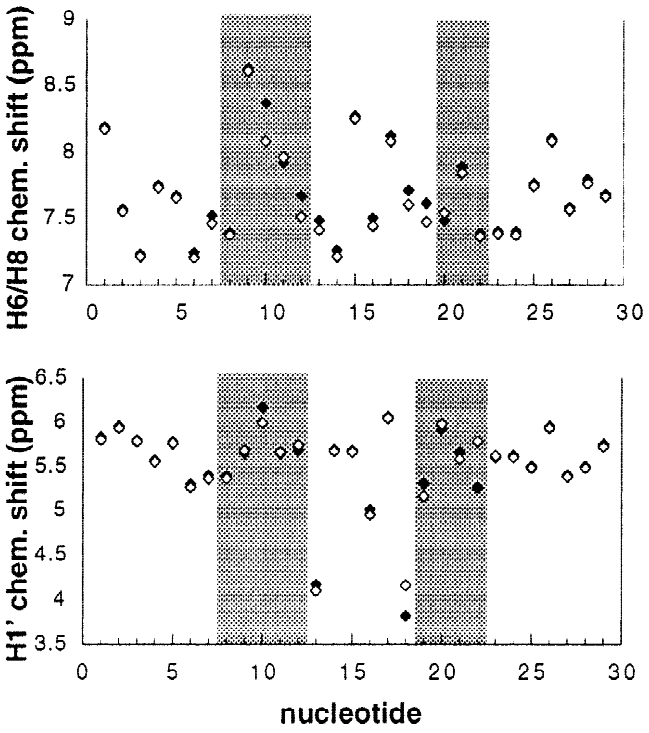

FIGURE 10. Comparison of chemical shift assignments for G10A and E73. Top graph shows the chemical shift values for resonances due to H8 and H6 protons of G10A and E73. Solid diamonds indicate G10A resonances; open diamonds indicate E73 resonances. Bottom graph shows the chemical shift values for H1′ resonances. Shaded regions indicate where assignments are less secure.

ought to have dire consequences. Recent mutational studies have called this reasoning into question. For example, G16 (E73 numbering), which is the "R" nucleotide in the SRL's GNRA tetraloop, can be replaced by a C (Tapprich & Dahlberg, 1990) or an A (Marchant & Hartley, 1994), and the CG pair (C13–G18) that closes that tetraloop can be replaced by a UG (Liu & Liebman, 1996). Substitutions like these have an impact on translational accuracy, but they are far from lethal. Even when G19 is replaced by a C, which should affect the formation of the SRL's cross-strand A stack, the only consequence is an approximate doubling of generation time, and a gradual loss of viability (Marchant & Hartley, 1994). Equally surprising, the AC that lies below the bulged G (A9–C22) can be replaced by many other pairs without effect on viability (O'Connor & Dahlberg, 1996). Finally, even G10, the bulged G itself, can be replaced by an A, with almost no change in growth rate (M. Macbeth & I. Wool, pers. comm.). Thus, it appears that at least 5 of the 12 conserved bases in the SRL cannot be making critical, base-specific interactions during protein synthesis; they are not "read."

The probable explanation of these findings is that it is the conformation of the SRL that counts, and that all the viable SRL mutants found so far leave its conformation largely intact. The insensitivity of ribosomes to base pair-conserving substitutions at C13–G19 is easy to understand. [It is less easy to rationalize why the double mutation that replaces C13–G18 with a GC (G13–C18) is not viable (Marchant & Hartley, 1994).] The ability of the SRL to tolerate mutations affecting G16 is also easily understood. Because the most important interaction of G16 is its stacking on A17, the only conformational consequence of replacing it by another nucleotide should be a modest destabilization of the SRL tetraloop.

The insensitivity of the SRL to substitutions at G19, and A9–C22 (PRO-SRL numbering) is more troubling. When G19 is replaced by a C, it is no longer possible for the SRL to form the type II AG that is a critical component of its cross-strand A stack. There is an AC pairing possible, however, that has approximately the same geometry, but it is far from isosteric. As for A9–C22 substitutions, contrary to the conclusion that O'Connor and Dahlberg (1996) drew from their mutational results, Watson–Crick base pairs cannot be accommodated at this position. The structure of the bulge requires that the two sides of the loop have parallel backbones at the 9–22 position, and Watson–Crick pairs have antiparallel backbones. Nevertheless, it may be possible to explain these mutations too. Crystallographic data indicate that the symmetric A9–A21 pair in E73 is less regular than the pairing proposed for its solution structure (C.C. Correll, A. Munishkin, Y.-L. Chan, Z. Ren, I.G. Wool, & T.A. Steitz, in prep.; Szewczak & Moore, 1995), and the PRO-SRL solution data suggest a juxtaposition that is not even a proper base pair, even though AC pairs that have the appropriate backbone symmetry are possible (Saenger, 1984). Evidently, it is unimportant how or even if the base at position 9 interacts with its neighbor as long as their backbone orientations are parallel. The data presented here provide direct evidence that the replacement of G10 with an A does not result in a major conformational reorganization.

Given the importance of the SRL for ribosome function, and the evidence that it is the conformation of the SRL that counts, it is surprising that an SRL mutation as destabilizing as the G10A mutation is tolerated in vivo. One way to explain it would be to postulate that the conformation of the SRL is stabilized by interactions with other parts of the ribosome, and hence that its intrinsic stability makes little difference, as long as its sequence is not incompatible with the "right" conformation. If this is so, then the hypothesis that Wool and his colleagues have advocated in the past, namely that the conformation of the SRL cycles during protein synthesis, deserves renewed scrutiny, but there are some restrictions that can be placed on it now that could not be placed on it before. If the conformation of the SRL is controlled by external interactions and it does not change during protein synthesis, then the conformation being stabilized must be the one that has been elucidated by X-ray crystallography and NMR

spectroscopy. Otherwise, it is impossible to explain why the SRL would be sensitive to ricin and alpha-sarcin in the intact ribosome, the way E73 is in vitro. Furthermore, for the same reason, if the conformation of the SRL cycles during protein synthesis, one of the conformations it adopts must be the one we have been talking about here.

Finally, there is the matter of the exchangeability of G10 H8. The rate of exchange of G10 8C-H in E73 and PRO-SRL is 10 times faster than the rate for GMP under identical conditions. This is a remarkable finding because all previous reports have indicated that the exchange rates of purine H8s in structured RNAs are never greater than those observed in random coils or free nucleotides. In double-stranded viral RNA, the rate of purine H8 exchange determined by tritium labeling is about 5 times slower than that of GMP, and the rates in individual nucleotides in tRNA and *E. coli* 5S rRNA range from 2 to 50 times slower than that of GMP (Gamble et al., 1976; Schoemaker et al., 1976; Farber & Cantor, 1981). In poly(rG)poly(rC), the rate determined by Raman spectroscopy was 10 times slower than the rate of free GMP (Benevides & Thomas, 1985).

H8 exchange is known to occur through an ylide mechanism in which N7 is protonated (Tomasz et al., 1972), and stabilization of that intermediate could facilitate exchange. However, both the C8 and N7 of G10 point directly into solution in the SRL. There is no evidence for bound metal ions in this part of the molecule or any hint of interactions with other parts of the SRL, and hence intermediate stabilization seems unlikely. We think it more likely that the abnormal chemical shift of G10 C1′ is related to the abnormal exchange properties of G10 H8. The H1′–H2′ coupling constant of E73 is larger than normal for a C2′ endo sugar (Szewczak & Moore, 1995), suggesting that an unusual sugar pucker for G10 could account for its C1′ chemical shift. The altered character of the sugar could propagate through the glycosydic bond to N9 and result in a lowering of the pK_a of C8, which would facilitate exchange.

MATERIALS AND METHODS

Samples

RNA samples were prepared using in vitro transcription by T7 RNA polymerase and gel purification. PRO-SRL was dialyzed into a buffer containing the following: 10 mM KH_2PO_4, 50 mM KCl, 15 mM NaCl, 0.5 mM EDTA, pH 7.6; the same buffer conditions were used for experiments on E73. G10A was dialyzed into a similar buffer: 10 mM KH_2PO_4, 75 mM KCl, 15 mM NaCl, 0.5 mM EDTA, pH 6.5.

UV melts

UV absorbance melting curves were collected at 260 nm from 5 to 95 °C on the Varian Cary 3E spectrophotometer. After in vitro transcription and gel purification, the E73, PRO-SRL, and G10A samples were dialyzed into the PRO-SRL NMR buffer described above, concentrated, and then diluted to 10, 1, and 0.5 OD/mL. Melting curves were recorded for each sample at all three concentrations to determine if melting behavior depended on concentration, which it would if oligonucleotides were dimerizing. The absorbance and temperature data were processed using the program Kaleidagraph. The MeltFit/PPC.out program written by David Draper was used to represent melting curves as sums of two-state transitions. It returns: ΔA_i, the hyperchromicity or amplitude of change in absorbance; ΔH_i, the enthalpy of unfolding; and T_{mi}, the melting temperature for each transition identified (Marky & Breslauer, 1987; Draper & Gluick, 1995).

NMR

Homonuclear and heteronuclear NMR experiments were performed on a Varian Unity v500 spectrometer, a Varian Unity+ v600 spectrometer, a GE W500 spectrometer, or a Bruker 490 spectrometer. NOESY experiments in H_2O were done using either GE jump-return spin echo or water-flip watergate sequences for H_2O suppression, with a mixing time of 150 ms. D_2O NOESY spectra were taken with mixing times of 50, 75, 150, or 300 ms. The pulse sequences and parameters were otherwise the same as described in Dallas and Moore (1997) and Stallings and Moore (1997).

Structure calculations

The calculations used to obtain a structure for PRO-SRL were performed using a modified TAMD algorithm (Stallings & Moore, 1997). Interproton distance and dihedral angle restraints typical of A-form RNA were used for the stem of the molecule: residues G1–G5, C25–C29, whereas relaxed distance and dihedral A-form restraints were used for C6 and G24. The distance restraints for the remainder of the molecule (residues C6–G24) were estimated from the intensities of crosspeaks in NOESY spectra, using the same criteria described in Dallas and Moore (1997). The dihedral angle restraints for the backbone of residues U7–C23 were as follows: α, β, γ, and ζ were not specified, ϵ was 200 ± 40 or ± 50 for U11–G14 and G19–C23, whereas ϵ was −120 ± 120 for U7–G10 and A15–G18. Pseudorotation angles typical of 2′ endo sugars were used for A9 and G10, and not specified for A15–A17. In other loop residues, values typical of 3′ endo sugar puckering were used. The glycosidic angle, χ, was *anti* for all residues, but allowed a more relaxed range in C6–G24. Weak planarity restraints (15 kcal mol^{-1} A^{-2}) were used for base pairs in the stem residues G1–G5 and C29–C25, and for base pairs A12–G19, C13–G18, and G14–A17 in the loop.

Exchange rate measurements

Pseudo first-order rate constants for H8 exchange were estimated from the slopes of plots of ln(*I*/*Io*) versus time, where *I* is a resonance strength at time *t* and *Io* is the strength of the same resonance at time zero. Resonance intensities were estimated by integrating resonances in NMR spectra (Brandes & Ehrenberg, 1986). The rate of H8 exchange in GMP was

determined by incubating samples of GMP in the NMR buffer used for PRO-SRL at 60, 70, and 80 °C for intervals of 30 or 60 min. One-dimensional proton spectra were then recorded at 25 °C, and H8 resonances were integrated. The rate of G10 H8 exchange in E73 was determined by measuring the change in the strength of the G10 H1′-G10 H8 NOESY peak in spectra taken over the course of several months. For purposes of analysis, it was assumed that exchange occurred only when the sample was at 30 °C, not when it was stored at 5 °C between experiments. Resonance strengths were normalized using the A15 H8–H1′ crosspeak as a reference. The rate of G10 H8 exchange in PRO-SRL was determined by collecting five constant-time HMQC spectra (Marino et al., 1997) over the course of 125 h, during which time the sample was maintained continuously at 30 °C. The strength of the G10 H8 crosspeak was normalized using the A26 H2 crosspeak as a reference.

ACKNOWLEDGMENTS

We thank Professor Ira Wool and Dr. Yuen-Ling Chan for providing us with our first sample of G10A, and for advice and encouragement. We are indebted to Professor Wool, Dr. Mark Macbeth, and Dr. Alex Szewczak for their helpful comments on this manuscript. We thank Dr. Sarah Stallings for invaluable technical assistance with the TAMD structural calculations of PRO-SRL. This work was supported by a grant from the NIH (GM-41651).

Received May 14, 1998; returned for revision June 8, 1998; revised manuscript received June 30, 1998

REFERENCES

Benevides JM, Thomas GJ Jr. 1985. Dependence of purine 8C-H exchange on nucleic acid conformation and base-pairing geometry: A dynamic probe of DNA and RNA secondary structures. *Biopolymers 24*:667–682.

Brandes R, Ehrenberg A. 1986. Kinetics of the proton–deuteron exchange at position H8 of adenine and guanine in DNA. *Nucleic Acids Res 14*:9491–9508.

Correll CC, Freeborn B, Moore PB, Steitz TA. 1997. Metals, motifs, and recognition in the crystal structure of a 5S rRNA domain. *Cell 91*:705–712.

Dallas A, Moore PB. 1997. The loop E–loop D region of *Escherichia coli* 5S rRNA: The solution structure reveals an unusual loop that may be important for binding ribosomal proteins. *Structure 5*:1639–1653.

Draper DE, Gluick TC. 1995. Melting studies of RNA unfolding and RNA–ligand interactions. *Methods Enzymol 259*:281–305.

Endo Y, Tsurugi K. 1988. The RNA *N*-glycosidase activity of ricin A-chain. *J Biol Chem 263*:8735–8739.

Endo Y, Wool IG. 1982. The site of action of α-sarcin on eukaryotic ribosomes. *J Biol Chem 257*:9054–9060.

Farber NM, Cantor CR. 1981. A slow tritium exchange study of the solution structure of *Escherichia coli* 5S ribosomal RNA. *J Mol Biol 146*:223–239.

Fernandez-Puentes C, Vazquez D. 1977. Effects of some proteins that inactivate eukaryotic ribosomes. *FEBS Lett 78*:143–146.

Gamble RC, Schoemaker HJP, Jekowsky E, Schimmel PR. 1976. Rate of tritium labeling of specific purines in relation to nucleic acid and particularly transfer RNA conformation. *Biochemistry 13*:2791–2799.

Gluck A, Endo Y, Wool IG. 1992. Ribosomal RNA identity elements for ricin A-chain recognition and catalysis. Analysis with tetraloop mutants. *J Mol Biol 226*:411–424.

Gluck A, Wool IG. 1996. Determination of the 28S ribosomal RNA identity element (G4319) for alpha-sarcin and the relationship of recognition to the selection of the catalytic site. *J Mol Biol 256*:838–848.

Heus HA, Pardi A. 1991. Structural features that give rise to the unusual stability of RNA hairpins containing GNRA loops. *Science 253*:191–194.

Lane MJ, Thomas GJ Jr. 1979. Kinetics of hydrogen-deuterium exchange in guanosine 5′-monophosphate and guanosine 3′:5′-monophosphate determined by laser-Raman spectroscopy. *Biochemistry 18*:3839–3846.

Liu R, Liebman SW. 1996. A translational fidelity mutation in the universally conserved sarcin/ricin domain of 25S yeast ribosomal RNA. *RNA 2*:254–263.

Marchant A, Hartley MR. 1994. Mutational studies on the α-sarcin loop of *Escherichia coli* 23S ribosomal RNA. *Eur J Biochem 226*:141–147.

Marino JP, Diener JL, Moore PB, Griesinger C. 1997. Multiple-quantum coherence dramatically enhances the sensitivity of CH and CH_2 correlations in uniformly ^{13}C-labeled RNA. *J Am Chem Soc 119*:7361–7366.

Marky LA, Breslauer KJ. 1987. Calculating thermodynamic data for transitions of any molecularity from equilibrium melting curves. *Biopolymers 26*:1601–1620.

Munishkin A, Wool IG. 1997. The ribosome-in-pieces: Binding of elongation factor EF-G to oligoribonucleotides that mimic the sarcin/ricin and thiostrepton domains of 23S ribosomal RNA. *Proc Natl Acad Sci USA 94*:12280–12284.

Nierhaus KH, Schilling-Bartetzko S, Twardowski T. 1992. The two main states of the elongating ribosome and the role of the α-sarcin stem-loop structure of 23S RNA. *Biochimie 74*:403–410.

O'Connor M, Dahlberg AE. 1996. The influence of base identity and base pairing on the function of the α-sarcin loop of 23S rRNA. *Nucleic Acids Res 24*:2701–2705.

Saenger W. 1984. *Principles of nucleic acid structure*. New York: Springer-Verlag.

Schoemaker HJP, Gamble RC, Budzik GP, Schimmel PR. 1976. Comparison of isotope labeling patterns of purines in three specific transfer RNAs. *Biochemistry 15*:2800–2803.

Stallings SC, Moore PB. 1997. The structure of an essential splicing element: Stem loop IIa from yeast U2 snRNA. *Structure 5*:1173–1185.

Stein EG, Rice LM, Brunger AT. 1997. Torsion angle molecular dynamics: A new, efficient tool for NMR structure calculation. *J Magn Reson B 127*:154–157.

Szewczak AA, Moore PB. 1995. The sarcin/ricin loop, a modular RNA. *J Mol Biol 247*:81–98.

Szewczak AA, Moore PB, Chan YL, Wool IG. 1993. The conformation of the sarcin/ricin loop from 28S ribosomal RNA. *Proc Natl Acad Sci USA 90*:9581–9585.

Tapprich WE, Dahlberg AE. 1990. A single base mutation at position 2661 in *E. coli* 23S ribosomal RNA affects the binding of ternary complex to the ribosome. *EMBO J 9*:2649–2655.

Tomasz M, Olson J, Mercado CM. 1972. Mechanism of the isotopic exchange of the C-8 hydrogen of purines in nucleosides and in deoxyribonucleic acid. *Biochemistry 11*:1235–1241.

Wimberly B, Varani G, Tinoco I Jr. 1993. The conformation of loop E of eukaryotic 5S ribosomal RNA. *Biochemistry 32*:1078–1087.

Wool IG, Gluck A, Endo Y. 1992. Ribotoxin recognition of ribosomal RNA and a proposal for the mechanism of translocation. *Trends Biochem Sci 17*:266–269.